MicroRNA-210-5p Alleviates Cardiac Fibrosis via Targeting Transforming Growth Factor-beta Type I Receptor in Rats on High Salt Diet

Kun Zhao
The First Affiliated Hospital with Nanjing Medical University
Yukang Mao
The First Affiliated Hospital with Nanjing Medical
Xiaoman Ye
Fourth Affiliated Hospital of Harbin Medical University
Jiazheng Ma
The First Affiliated Hospital with Nanjing Medical University
Litao Sun
Southeast University
Peng Li
The First Affiliated Hospital with Nanjing Medical University
Yong Li (liyongmydream@126.com)
The First Affiliated Hospital with Nanjing Medical University https://orcid.org/0000-0002-9619-1694

Research

Keywords: high salt diet, cardiac fibrosis, cardiac fibroblasts, microRNA-210-5p, transforming growth factor-beta type I receptor

Posted Date: March 2nd, 2021

DOI: https://doi.org/10.21203/rs.3.rs-243221/v1

Abstract

Background: The aim of the present study was to explore whether high salt diet (HSD) caused cardiac fibrosis regardless of blood pressure in rats, and to determine the effects of microRNA (miR)-210-5p on sodium chloride (NaCl)-induced fibrosis in neonatal rat cardiac fibroblasts (NRCFs) and its target.

Methods: The rats received 8% HSD *in vivo*, and NRCFs were treated with NaCl *in vitro*.

Results: The levels of collagen I, alpha-smooth muscle actin (α-SMA) and transforming growth factor-beta (TGF-β) were increased in the heart of hypertension (HTN), hypertension-prone (HP) and hypertension-resistant (HR) rats on HSD. Middle and high doses (50 mM and 100 mM) of NaCl increased the levels of collagen I, α-SMA and TGF-β in NRCFs. The expression level of miR-210-5p was reduced in NaCl-treated NRCFs by miR high-throughput sequencing. The NaCl-induced increases of collagen I, α-SMA and TGF-β were inhibited by miR-210-5p agomiR, and further enhanced by miR-210-5p antagomiR. Bioinformatics analysis and luciferase reporter assays demonstrated that TGF-β type I receptor (TGFβRI) was a direct target gene of miR-210-5p. These results indicated that HSD resulted in cardiac fibrosis regardless of blood pressure.

Conclusion: The upregulation of miR-210-5p could attenuate NRCF fibrosis via targeting TGFβRI. Thus, upregulating miR-210-5p to inhibit TGF-β signaling pathway might be a strategy for the treatment of cardiac fibrosis.

Introduction

Epidemiological studies have reported the association between high salt intake and the risk of cardiovascular diseases [1-3]. High sodium or salt intake can lead to chronic comorbidities such as hypertension, heart failure, stroke, chronic kidney disease, and increase mortality [4, 5]. Salt sensitive rodent models demonstrate heart failure subsequent to pathological left ventricle remodeling with high Na^+ [6].

Myocardial fibrosis is characterized by an excessive deposition of extracellular matrix proteins in the heart. Although fibrosis formation is initially reparative, on-going and excessive myocardial fibrosis in the long term may lead to arrhythmia, cardiac wall stiffening, and subsequently heart failure [7]. High salt diet (HSD) can induce hypertension and cardiac remodeling in Dahl salt-sensitive rats [8]. HSD markedly accelerates cardiac damage by stimulating the cardiac renin-angiotensin system under higher blood pressure [9]. Investigations have already revealed that volume overload and/or increased blood pressure secondary to salt overload can exert detrimental effects on the function of artery wall [10]. Evidence also implies that high salt intake may adversely impact the vascular wall—regardless of blood pressure [11]. However, whether high salt intake can cause cardiac fibrosis regardless of blood pressure is not clear.

MicroRNAs (miRs), a group of small and non-coding RNAs, negatively regulate gene expression via promoting messenger RNA (mRNA) degradation or blocking mRNA translation [12-15]. Many miRs have

been recognized as biomarkers and possible targets for the diagnosis or therapy of some diseases [16]. MicroRNA-210 expression is altered in cardiovascular diseases, such as acute myocardial infarction, atherosclerosis, aortic stenosis, preeclampsia and heart failure. The overexpression of miR-210 exerts protective effects on target organs in some of these diseases [17]. Here, we aimed to explore the effect of miR-210-5p on NaCl-induced fibrosis of heart and its mechanism.

Materials And Methods

Animals

The experiments were carried out using male Sprague-Dawley (SD) rats weighing 160-180 g (Vital River Biological Co., Ltd, Beijing, China). Approved by the Experimental Animal Care and Use Committee of Nanjing Medical University, all procedures were conducted in accordance with the Guide for the Care and Use of Laboratory Animals (NIH publication No. 85-23, revised in 1996). The rats were kept in a temperature-controlled room on a 12-h light-dark cycle with free access to standard chow and tap water. The study was approved by the ethics committee of Nanjing Medical University.

Rats on HSD

Male SD rats weighing 160-180 g were randomly divided into the control diet (CD, 0.4% NaCl) group and the HSD (8% NaCl, Research Diets Inc., NJ, USA) group and fed for 8 weeks. The rats with systolic blood pressure (SBP)≥150 mm Hg were defined as hypertension (HTN) rats, those with SBP between 130 and 150 mm Hg as hypertension-prone (HP) rats, and those with SBP□130 mm Hg as hypertension-resistant (HR) rats. HR and HP rats were taken as NonHTN rats.

Measurement of tail artery blood pressure

Blood pressure was measured weekly in the tail of the conscious rat using a noninvasive computerized tail-cuff system (Kent Scientific Corporation, CT, USA). The rat was warmed at 35°C for 10-20 min before measurement to achieve a steady pulse and allow for the detection of tail artery pulsation. To minimize stress-induced fluctuations, the rat was pre-trained by daily blood pressure measurement for at least 1 week before the initiation of the experiments. The systolic blood pressure (SBP), diastolic blood pressure (DBP), and mean artery pressure (MAP) of tail artery were obtained by averaging at least 10 measurements [18].

Culturing of CFs isolated from neonatal rats

Primary cardiomyocytes were isolated from 1- to 2-day-old newborn SD rats (Vital River Biological Co., Ltd., Beijing, China). The heart was excised and digested through agitations in buffer containing collagenase type II (Worthington Biochemical Corp., NJ, USA) and pancreatin (Sigma, MO, USA). The atria and great vessels were discarded. The ventricles were cut into small pieces and digested with collagenase type II and pancreatin. Cells from digestion were collected, cultured in complete Dulbecco's

modified Eagle's medium (Biochannel Biotechnology Co., Ltd.) for 2-4 hours to reduce fibroblasts, and then enriched for cardiomyocytes. The cardiomyocytes were cultured at 37°C with 5% CO_2 and 95% air.

High-throughput small RNA sequencing (sRNA-seq)

High-throughput sRNA-seq was conducted by Biomarker Technologies Co., Ltd (Beijing, China). In brief, total RNA from three pairs of NRCFs (50-100 mg) was isolated using TRIzol (Invitrogen Life Technologies, Carlsbad, CA). RNA concentration and purity were detected by the NanoDrop 2000 Spectrophotometer (Thermo Fisher Scientific, Wilmington, DE). RNA integrity was assessed using the RNA Nano 6000 Assay Kit of the Agilent Bioanalyzer 2100 System (Agilent Technologies, CA, USA). When the detection results met the requirements, the library for sRNA sequencing was constructed using NEBNextR UltraTM small RNA Sample Library Prep Kit for IlluminaR (NEB, USA). The clustering of the index-coded samples was performed on a cBot ClustermGeneration System using TruSeq PE Cluster Kitv3-cBot-HS (Illumia). Finally, the Agilent Bioanalyzer 2100 platform was used for sequencing, and a large number of high-quality raw data were produced. Then, low-quality reads containing adapter or ploy-N were removed from raw data by cutadapt software. All the downstream analyses were based on clean data with high quality. The differential expression analyses in our study were performed with DESeq R package based on binomial distribution, and combined with Fisher's exact test and likelihood ratio test. The resulting P values were adjusted using Benjamini and Hochberg's approach for controlling the false discovery rate. Target genes with an adjusted P-value <0.01 and absolute value of log2 (Fold change) >1 found by DESeq were assigned as differentially expressed (False Discovery Rate (FDR) <0.01). Gene Ontology (GO) and Kyoto Encyclopedia of Genes and Genomes (KEGG) pathway enrichment analysis of the target genes with differentially expressed miRNAs were implemented using clusterProfiler R packages.

Cell transfection

Transfection of miR-210-5p agomir/antagomir/scrambled controls (RiboBio, Guangzhou, China) was initiated using Lipofectamine RNAiMAX (Invitrogen, Carlsbad, CA, USA). Transfection procedures were carried out when the cells were 50% confluent. After 48 hours, the cells received other treatments or were scratched.

Western blotting

Rats were anesthetized with isoflurane (3.5%) and sacrificed after receiving HSD for 8 weeks. The hearts were removed, immediately frozen in liquid nitrogen and stored at −70 ℃ until use. Heart tissues or cultured cells were sonicated in RIPA lysis buffer and homogenized. The debris was removed and the supernatant was obtained after centrifugation at 12,000 g for 10 min at 4°C. About 30-50 μg proteins was loaded for electrophoresis, and probed with primary antibodies against collagen I (1:1000; No.14695-1-AP; Proteintech Co., Wuhan, China), α-SMA (1:1000; No.14395-1-AP; Proteintech Co.), TGF-β (1:1000; No.21898-1-AP; Proteintech Co.). GAPDH (1:1000, AF0006; Beyotime Biotechnology Co., Shanghai, China) was used as internal control. Images were analyzed using the Image-Pro Plus software.

Quantitative real time-PCR (qRT-PCR)

The total RNA in samples was extracted with TRIzol (Ambion, TX, USA). The cDNA was extracted from RNA with reverse transcription using random primers in a total volume of 10 μL according to the instructions of the PrimeScript™ RT Master Mix (TaKaRa Biomedical Technology, Beijing, China). All cDNA was stored at − 80 °C before use. mRNA was determined with SYBR Green I fluorescence. All samples were amplified in triplicates for 40 cycles in 384-well plates. The relative gene expression was determined by calculating the values of Δcycle threshold (ΔCt) as a relative quantity to the endogenous control. The primers (Genscript, Nanjing, China) are shown in Table S1. Bulge-loop^{TM} miRNA qRT-PCR Primer Sets (one RT primer and a pair of qPCR primers for each set) specific for miR-210-5p was designed by RiboBio (Guangzhou, China). The miRs from rat serum were extracted using miRNeasy Serum/Plasma Kit (217184, Qiagen Co., Germany).

Statistical analyses

Data were presented as mean ± standard error of the mean (SEM). Using GraphPad Prism 7.0 (GraphPad software Inc., CA, USA), statistical significance among multiple groups was evaluated by one-way analysis of variance (ANOVA) with the Bonferroni post-hoc test. A two-tailed P-value <0.05 was considered statistically significant.

Results

Effects of HSD on cardiac fibrosis in the rats

Based on blood pressure, the HSD rats were divided into HR, HP and HTN groups. Among the 60 HSD rats, 25 (41.67%) were NonHTN (HR+HP) rats, and 35 were (58.33%) HTN rats. Among the NonHTN rats, 12 (20.00%) were HP rats, and 13 (21.67%) were HR rats (Table S2). SBP, DBP and MAP were higher in HP and HTN rats compared with CD or HP rats (Figure S1). The body weight and food intake of HR, HP and HTN rats on HSD were lower compared with CD rats (Figure S2). The fibrosis levels of the heart in HR, HP and HTN rats on HSD were higher than that in CD rats by Masson's staining. This phenomenon was also observed in thoracic aorta and renal artery (Figure 1A). The mRNA expression levels of collagen I, α-SMA and TGF-β were increased in HR, HP and HTN rats on HSD (Figure 1B). The protein expression levels of collagen I, α-SMA and TGF-β were elevated in HR, HP and HTN rats on HSD (Figure 1C).

Effects of NaCl on NRCF fibrosis

The mRNA levels of collagen I, α-SMA and TGF-β were increased in NRCFs treated with middle (50 mM) and high (100 mM) doses of NaCl. In NRCFs, 25 mM NaCl and mannitol (100 mM) exerted no effect on the mRNA levels of collagen I, α-SMA and TGF-β (Figure 2A). Middle (50 mM) and high (100 mM) doses of NaCl increased the protein levels of collagen I, α-SMA and TGF-β in NRCFs. Low dose of NaCl (25 Mm) and mannitol (100 mM) had no effect on the protein expression levels of collagen I, α-SMA and TGF-β (Figure 2B). Middle dose of NaCl (50 mM) was used in the following experiments.

Conjoint analyses of sRNA-seq data

sRNA-seq was performed to determine the effects of high salt on the miRNA expression of NRCFs. After the credible normalization and standardization of raw data shown in the box-plot (Figure 3A), we found 348 significantly differenced miRNAs. As shown in Figure 3B-C, we found 262 significantly up-regulated miRNAs and 86 down-regulated miRNAs in high salt-treated NRCFs compared to the control group (|FC|>=2, FDR<0.01). The M-versus-A (MA) plot visualized the variation of all the miRNAs among samples of the two groups (Figure 3D). The up-regulated miRNAs were marked red, while the down-regulated miRNAs were marked green (Figure 3D).

Next, we performed the GO and KEGG pathways analyses of target genes of differentially expressed miRNAs between high-salt and control groups, which were apparently associated with various functional processes and pathways (Figure 4A-B). The top 10 enriched terms of KEGG pathways (Figure 4B), biological process (Figure 4C-D), molecular function (Figure 4E-F), and cellular component (Figure 4G-H) were shown in the corresponding enriched barplot and dotplot, respectively. The size of the dot represented the number of target genes of differentially expressed miRNA, while the color of the dot represented the corrected P-value of the hypergeometric test.

The expressions of the top 10 down-regulated miRs (miR-99a-3p, miR-6328, miR-217-5p, miR-210-5p, miR-223-3p, miR-195-3p, miR-181b-1-3p, miR-760-3p, miR-877, miR-142-5p) in NRCFs induced by NaCl were shown in Table 1.

Effects of miR-210-5p on NaCl-induced fibrosis of NRCFs

The expression level of miR-210-5p was reduced in NRCFs treated with NaCl. The level of miR-210-5p was reduced in the heart of HR, HP and HTN rats on HSD. The level of miR-210-5p was reduced in the serum of HR, HP and HTN rats on HSD (Figure 5A). The agomiR of miR-210-5p administration increased the level of miR-210-5p in NRCFs treated with PBS or NaCl (Figure S3A). The level of miR-210-5p was reduced in NRCFs treated with PBS or NaCl after the administration of miR-210-5p antagomiR (Figure S3B). The mRNA levels of collagen I, α-SMA and TGF-β were increased in NRCFs treated with NaCl, and these increases were inhibited after miR-210-5p agomiR treatment (Figure 5B). The protein levels of collagen I, α-SMA and TGF-β were increased in NRCFs treated with NaCl, which was reversed after miR-210-5p agomiR administration (Figure 5C). The administration of miR-210-5p antagomiR significantly increased the mRNA levels of collagen I, α-SMA and TGF-β in RNCFs. MiR-210-5p antagomiR further enhanced the NaCl-induced increases of collagen I, α-SMA and TGF-β mRNA levels in NRCFs (Figure 5D). Treatment with miR-210-5p antagomiR markedly increased the protein levels of collagen I, α-SMA and TGF-β in RNCFs. The NaCl-induced increases of collagen I, α-SMA and TGF-β protein levels were further enhanced by miR-210-5p antagomiR treatment in NRCFs (Figure 5E).

The target of miR-210-5p

A bioinformatics analysis of the predicted interactions was performed between miR-210-5p and the target mRNAs from Targetscan. We found that TGFβRI was a potential target gene of miR-210-5p. The schematic showed the comparison between the rat 3'UTR regions of the TGFβRI gene and miR-210-5p. There are four potential binding sites of TGFβRI, including 898-904, 1339-1346, 2871-2877 and 2898-2904 TGFβRI 3' UTR (Figure 6A). MiR-210-5p significantly decreased the luciferase activities of the vector with the wild type TGFβRI 3'UTR compared with NC miR, and this decrease was attenuated by TGFβ1R MUT1 (898-904, 6.79%), TGFβ1R MUT2 (1339-1346, 19.52%), TGFβ1R MUT3 (2871-2877, 14.41%) and TGFβ1R MUT4 (2898-2904, 23.73%) (Figure 6B). TGFβRI mRNA expression level was increased in CFs treated with NaCl. The level of TGFβRI mRNA was reduced by miR-210-5p agomiR administration (Figure 6C). TGFβRI protein level was increased in CFs treated with NaCl. The level of TGFβRI protein was reduced by miR-210-5p agomiR treatment (Figure 6D). The inhibiting effect of miR-210-5p agomiR on the increases of collagen I, α-SMA and TGF-β in RNCFs was reversed by SRI-011381, an activator of TGF-β signaling pathway (Figure 6E).

Discussion

We currently found that HSD caused cardiac fibrosis regardless of blood pressure. The fibrosis of the heart was increased in the normotensive rats receiving HSD. The fibrosis was enhanced in NRCFs treated with NaCl. The expression level of miR-210-5p was increased in NaCl-treated NRCFs as shown by miRNA sequencing. Treatment with miR-210-5p agomiR alleviated NaCl-induced fibrosis of NRCFs, but the administration of miR-210-5p antagomiR further deteriorated NaCl-induced fibrosis of NRCFs. The upregulation of miR-210-5p ameliorated the fibrosis of cardiac fibroblasts via targeting TGFβ1R directly.

HSD can cause hypertension, as well as cardiac and renal fibrosis in salt-sensitive hypertensive rats [8]. High salt intake is associated with a hypertensive response accompanied by the development compensatory hypertrophy of left ventricular and the decompensated congestive heart failure [19]. High sodium intake increases blood pressure, cardiovascular mortality, the overall cardiovascular adverse outcomes and remodeling of heart [20]. A previous study showed that high salt intake caused cardiac hypertrophy without significantly increasing blood pressure in rats receiving an 8-week HSD [21]. It is unusual that an 8-week HSD failed to produce any increase in blood pressure. In our present study, based on the blood pressure, we divided the HSD rats into HR (SBP□130 mm Hg), HP (SBP between 130 and 150 mm Hg) and HTN (SBP≥150 mm Hg) groups. The fibrosis of heart, thoracic aorta, and renal artery was increased in rats of all three groups compared to control rats. The expression levels of collagen I, α-SMA and TGF-β were elevated in HR, HP and HTN rats on HSD. These results indicated that high salt intake produced cardiac fibrosis regardless of blood pressure. High salt intake could induce fibrosis of the heart not only in rats with hypertension but also in those with normotension.

We next incubated NRCFs with NaCl to simulate high salt condition of cardiac fibroblasts *in vitro*. The expression levels of collagen I, α-SMA and TGF-β were enhanced in NaCl-treated NRCFs. We found that the same concentration of mannitol, an osmotic stress control of NaCl [22, 23], did not affect the

expression levels of collagen I, α-SMA and TGF-β in NRCFs. Our results suggested that the effect of NaCl in inducing fibrosis of cardiac fibroblasts was not mediated by osmolarity but itself.

It has been reported that several miRs were involved in the modulation of cardiac fibrosis [24-26]. Growing evidence showed that miRs could be useful diagnostic and prognostic biomarkers or therapeutic targets of cardiovascular diseases due to their involvement in the pathophysiological processes as well as their stability in urine and blood [27-29]. We presently found that miR-210-5p expression level was reduced in NaCl-treated NRCFs by miRs high-throughput sequencing, and this decrease was verified by RT-PCR. In addition, we found that the miR-210-5p levels were reduced in the serum and heart of rats on HSD. The results indicated that miR-210-5p might be a diagnostic and prognostic biomarker of cardiac fibrosis. We hypothesized that miR-210-5p might regulate the high salt-induced fibrosis of cardiac fibroblasts.

A previous study showed that the upregulation of miR-210 could promote myocardium angiogenesis in rats with acute myocardial infarction [30]. The overexpression of miR-210 could attenuate the oxygen-glucose deprivation/reperfusion-induced cardiomyocyte damage, while the decrease of miR-210 expression could aggravate the apoptosis of cardiomyocytes [31]. However, the roles of miR-210-5p in cardiovascular diseases, especially cardiac remodeling, remain unclear. To ascertain the role of miR-210-5p in regulating high salt-induced heart fibrosis, miR-210-5p agomiR and antagomiR were used to up- or down-regulate miR-210-5p level in cardiac fibroblasts in this study. The results showed that treatment with miR-210-5p agomiR increased the level of miR-210-5p in NRCFs treated with PBS or NaCl, while the administration of miR-210-5p antagomiR reduced the level of miR-210-5p in NRCFs treated with PBS or NaCl. Treatment with miR-210-5p agomiR inhibited the NaCl-induced increases of collagen I, α-SMA and TGF-β in NRCFs. In addition, miR-210-5p antagomiR administration further enhanced the NaCl-induced increases of collagen I, α-SMA and TGF-β in NRCFs. These results demonstrated that the upregulation of miR-210-5p could alleviate heart fibrosis, while the downregulation of miR-210-5p could deteriorate heart fibrosis. Therefore, miR-210-5p is a potential therapeutic target of cardiac fibrosis.

TGF-β, a fibrogenic growth factor, triggers fibrogenic signaling cascades through binding to surface receptors, and activating the downstream signaling cascades [32]. TGF-β produces biological effects via two types of receptors: TGF-β type I receptor (TGFβRI) and TGF-β type II receptor (TGFβRII) [33]. MiRs promote mRNA degradation via direct binding to the target mRNAs to negatively regulate gene expressions [34, 35]. Bioinformatics analysis by Targetscan illustrated that TGFβRI was a potential target gene of miR-210-5p. The level of TGFβRI was increased in NaCl-treated NRCFs, and this increase was alleviated by miR-210-5p agomiR. SRI-011381, an activator of TGF-β signaling pathway, reversed the alleviating effects of miR-210-5p agomiR on the NaCl-induced increases of collagen I, α-SMA and TGF-β in NRCFs. The schematic showed four potential binding sites of TGFβRI to miR-210-5p: 898-904, 1339-1346, 2871-2877 and 2898-2904 of TGFβRI 3' UTR. MiR-210-5p significantly decreased the luciferase activities of the vector with wild type TGFβRI 3'UTR, and this decrease was reversed by 1339-1346, 2871-2877 and 2898-2904 mutation, and most obviously by 2898-2904 mutation. These data indicated that TGFβRI could be the direct target of miR-210-5p. The 2898-2904 sequence of TGFβRI 3'UTR might be the

most possible binding site of miR-210-5p. MiR-210-5p could alleviate the fibrosis of cardiac fibroblasts via downregulating TGFβRI transcription.

In conclusion, high salt intake induces cardiac fibrosis regardless of blood pressure. The expression of miR-210-5p is downregulated in the heart of rats with high sodium intake. The upregulation of miR-210-5p significantly ameliorates high salt-induced heart fibrosis via targeting TGFβRI directly. The 2898-2904 sequence of TGFβRI 3'UTR is the most possible binding site of miR-210-5p. MiR-210-5p may be a diagnostic and prognostic biomarker or a therapeutic target of cardiac fibrosis.

Abbreviations

α-SMA: alpha-smooth muscle actin; CD: control diet; DBP: diastolic blood pressure; HP: hypertension-prone; HR: hypertension-resistant; HSD: high salt diet; HTN: hypertension; MAP: mean artery pressure; miR: microRNA; NaCl: sodium chloride; NRCFs: neonatal rat cardiac fibroblasts; SBP: systolic blood pressure; SD: Sprague-Dawley; SEM: standard error of the mean; TGF-β: transforming growth factor-beta; TGFβRI: TGF-β type I receptor.

Declarations

Acknowledgements

Not applicable.

Authors' contributions

KZ performed all experiments. YKM XMY JZM, and LTS participated in data analysis, carried out sequence alignments. KZ and PL drafted the manuscript. PL and YL designed the project, and revised the manuscript. All authors read and approved the final manuscript.

Funding

This work was supported by grants from the Priority Academic Program Development of Jiangsu Higher Education Institutions (No. 10231802)

Availability of data and materials

For original data, please contact corresponding author Yong Li, liyongmydream@126.com

Ethics approval and consent to participate

Animal studies were carried out under protocols approved by the Experimental Animal Care and Use Committee of Nanjing Medical University.

Consent for publication

Not applicable.

Competing interests

The authors declare no competing interests.

Author details

[1]Department of Cardiology, The First Affiliated Hospital of Nanjing Medical University, Nanjing, China. [2]Intensive Care Unit, The Fourth Affiliated Hospital of Nanjing Medical University, Nanjing, China. [3]SEU-FEI Nano-Pico Center, Key Laboratory of MEMS of Ministry of Education, Southeast University, Nanjing, 210096, China.

References

[1] D. Neupane, A. Rijal, M.E. Henry, P. Kallestrup, B. Koirala, C.S. McLachlan, K. Ghimire, D. Zhao, S. Sharma, Y. Pokharel, K. Joseph, M.H. Olsen, A.E. Schutte, L.J. Appel, Mean dietary salt intake in Nepal: A population survey with 24-hour urine collections, J Clin Hypertens (Greenwich), 22 (2020) 273-279.

[2] D. Malta, K.S. Petersen, C. Johnson, K. Trieu, S. Rae, K. Jefferson, J.A. Santos, M.M.Y. Wong, T.S. Raj, J. Webster, N.R.C. Campbell, J. Arcand, High sodium intake increases blood pressure and risk of kidney disease. From the Science of Salt: A regularly updated systematic review of salt and health outcomes (August 2016 to March 2017), J Clin Hypertens (Greenwich), 20 (2018) 1654-1665.

[3] Y. Xue, Q. Wen, C. Xu, X. Zhang, J. Zeng, A.M. Sha, C. Lan, L. Li, H. Wang, X. Yang, C. Zeng, Elevated Salt Taste Threshold Is Associated with Increased Risk of Coronary Heart Disease, J Cardiovasc Transl Res, (2020).

[4] Y. Patel, J. Joseph, Sodium Intake and Heart Failure, Int J Mol Sci, 21 (2020).

[5] D. Susic, E.D. Frohlich, Salt consumption and cardiovascular, renal, and hypertensive diseases: clinical and mechanistic aspects, Curr Opin Lipidol, 23 (2012) 11-16.

[6] A.C. Gomes, I. Falcao-Pires, A.L. Pires, C. Bras-Silva, A.F. Leite-Moreira, Rodent models of heart failure: an updated review, Heart Fail Rev, 18 (2013) 219-249.

[7] T.R. Eijgenraam, H.H.W. Sillje, R.A. de Boer, Current understanding of fibrosis in genetic cardiomyopathies, Trends Cardiovasc Med, 30 (2020) 353-361.

[8] C.M. Shea, G.M. Price, G. Liu, R. Sarno, E.S. Buys, M.G. Currie, J.L. Masferrer, Soluble guanylate cyclase stimulator praliciguat attenuates inflammation, fibrosis, and end-organ damage in the Dahl model of cardiorenal failure, Am J Physiol Renal Physiol, 318 (2020) F148-F159.

[9] Y. Hayakawa, T. Aoyama, C. Yokoyama, C. Okamoto, H. Komaki, S. Minatoguchi, M. Iwasa, Y. Yamada, I. Kawamura, M. Kawasaki, K. Nishigaki, A. Mikami, F. Suzuki, S. Minatoguchi, High salt intake damages the heart through activation of cardiac (pro) renin receptors even at an early stage of hypertension, PLoS One, 10 (2015) e0120453.

[10] O. Dumont, F. Pinaud, A.L. Guihot, C. Baufreton, L. Loufrani, D. Henrion, Alteration in flow (shear stress)-induced remodelling in rat resistance arteries with aging: improvement by a treatment with hydralazine, Cardiovasc Res, 77 (2008) 600-608.

[11] R. Agocs, D. Sugar, A.J. Szabo, Is too much salt harmful? Yes, Pediatr Nephrol, 35 (2020) 1777-1785.

[12] D.P. Bartel, MicroRNAs: genomics, biogenesis, mechanism, and function, Cell, 116 (2004) 281-297.

[13] M. Javadian, T. Gharibi, N. Shekari, M. Abdollahpour-Alitappeh, A. Mohammadi, A. Hossieni, H. Mohammadi, T. Kazemi, The role of microRNAs regulating the expression of matrix metalloproteinases (MMPs) in breast cancer development, progression, and metastasis, J Cell Physiol, (2018).

[14] E. van Rooij, The art of microRNA research, Circ Res, 108 (2011) 219-234.

[15] A.M. Mohr, J.L. Mott, Overview of microRNA biology, Semin Liver Dis, 35 (2015) 3-11.

[16] J.N. Jones Buie, A.J. Goodwin, J.A. Cook, P.V. Halushka, H. Fan, The role of miRNAs in cardiovascular disease risk factors, Atherosclerosis, 254 (2016) 271-281.

[17] Y. Guan, X. Song, W. Sun, Y. Wang, B. Liu, Effect of Hypoxia-Induced MicroRNA-210 Expression on Cardiovascular Disease and the Underlying Mechanism, Oxid Med Cell Longev, 2019 (2019) 4727283.

[18] C. Liu, C.X. Yang, X.R. Chen, B.X. Liu, Y. Li, X.Z. Wang, W. Sun, P. Li, X.Q. Kong, Alamandine attenuates hypertension and cardiac hypertrophy in hypertensive rats, Amino Acids, 50 (2018) 1071-1081.

[19] O.V. Fedorova, M.I. Talan, N.I. Agalakova, E.G. Lakatta, A.Y. Bagrov, Coordinated shifts in Na/K-ATPase isoforms and their endogenous ligands during cardiac hypertrophy and failure in NaCl-sensitive hypertension, J Hypertens, 22 (2004) 389-397.

[20] F. Nista, F. Gatto, M. Albertelli, N. Musso, Sodium Intake and Target Organ Damage in Hypertension-An Update about the Role of a Real Villain, Int J Environ Res Public Health, 17 (2020).

[21] Y. Takeda, T. Yoneda, M. Demura, I. Miyamori, H. Mabuchi, Sodium-induced cardiac aldosterone synthesis causes cardiac hypertrophy, Endocrinology, 141 (2000) 1901-1904.

[22] M. Liu, M. Deng, Q. Luo, X. Dou, Z. Jia, High-Salt Loading Downregulates Nrf2 Expression in a Sodium-Dependent Manner in Renal Collecting Duct Cells, Front Physiol, 10 (2019) 1565.

[23] D. Zhang, C. Wang, S. Cao, Z. Ye, B. Deng, A. Kijlstra, P. Yang, High-Salt Enhances the Inflammatory Response by Retina Pigment Epithelium Cells following Lipopolysaccharide Stimulation, Mediators

Inflamm, 2015 (2015) 197521.

[24] G. Sygitowicz, A. Maciejak-Jastrzebska, D. Sitkiewicz, MicroRNAs in the development of left ventricular remodeling and postmyocardial infarction heart failure, Pol Arch Intern Med, 130 (2020) 59-65.

[25] L. Medzikovic, L. Aryan, M. Eghbali, Connecting sex differences, estrogen signaling, and microRNAs in cardiac fibrosis, J Mol Med (Berl), 97 (2019) 1385-1398.

[26] M. Dutka, R. Bobinski, J. Korbecki, The relevance of microRNA in post-infarction left ventricular remodelling and heart failure, Heart Fail Rev, 24 (2019) 575-586.

[27] G. Condorelli, M.V. Latronico, G.W. Dorn, 2nd, microRNAs in heart disease: putative novel therapeutic targets?, Eur Heart J, 31 (2010) 649-658.

[28] R. Dumache, V. Ciocan, C. Muresan, A.F. Rogobete, A. Enache, Circulating MicroRNAs as Promising Biomarkers in Forensic Body Fluids Identification, Clin Lab, 61 (2015) 1129-1135.

[29] H.A. Cakmak, M. Demir, MicroRNA and Cardiovascular Diseases, Balkan Med J, 37 (2020) 60-71.

[30] J. Wang, Y. Zhang, Y.M. Liu, L.L. Guo, P. Wu, Y. Dong, G.J. Wu, Huoxue Anxin Recipe () promotes myocardium angiogenesis of acute myocardial infarction rats by up-regulating miR-210 and vascular endothelial growth factor, Chin J Integr Med, 22 (2016) 685-690.

[31] W.S. Bian, P.X. Shi, X.F. Mi, Y.Y. Sun, D.D. Yang, B.F. Gao, S.X. Wu, G.C. Fan, MiR-210 protects cardiomyocytes from OGD/R injury by inhibiting E2F3, Eur Rev Med Pharmacol Sci, 22 (2018) 743-749.

[32] N.G. Frangogiannis, Cardiac fibrosis, Cardiovasc Res, (2020).

[33] K. Tzavlaki, A. Moustakas, TGF-beta Signaling, Biomolecules, 10 (2020).

[34] J. Liu, F. Liu, The Yin and Yang function of microRNAs in insulin signalling and cancer, RNA Biol, 18 (2021) 24-32.

[35] S. Paul, L.M. Ruiz-Manriquez, S.J. Ledesma-Pacheco, J.A. Benavides-Aguilar, A. Torres-Copado, J.I. Morales-Rodriguez, M. De Donato, A. Srivastava, Roles of microRNAs in chronic pediatric diseases and their use as potential biomarkers: A review, Arch Biochem Biophys, 699 (2021) 108763.

Tables

Table 1. Top 10 down-regulated miRs expression in NRCFs treated with NaCl		
Gene name	Regulation	Fold change (log2)
miR-99a-3p	down	3.870048132
miR-6328	down	3.207486944
miR-217-5p	down	3.066557191
miR-210-5p	down	2.882367865
miR-223-3p	down	2.822900806
miR-195-3p	down	2.14808013
miR-181b-1-3p	down	2.105799477
miR-760-3p	down	2.055508252
miR-877	down	1.768360738
miR-142-5p	down	1.750054433

Figures

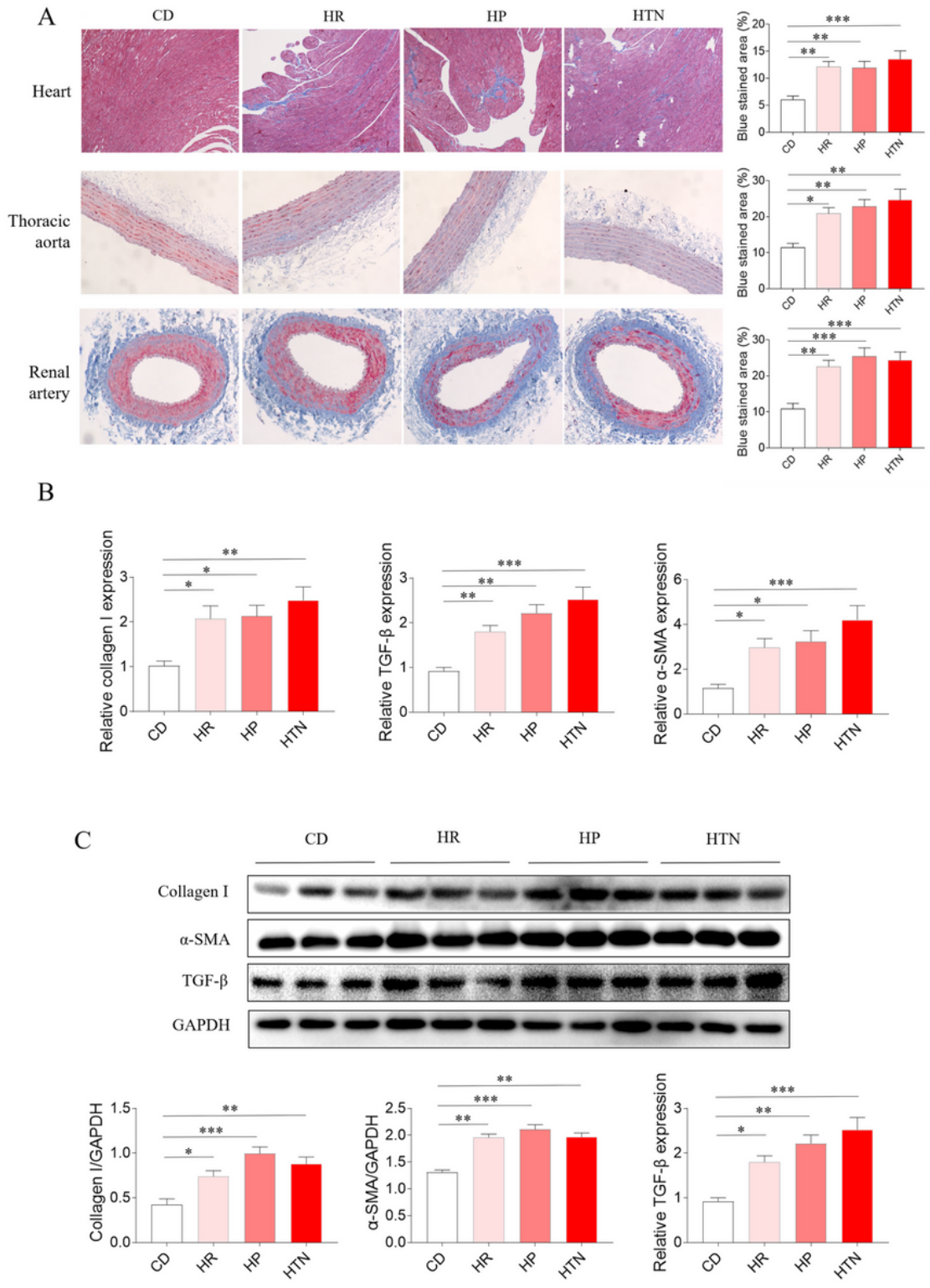

Figure 1

Effects of high salt diet (HSD) on cardiac fibrosis of rats. A, The levels of cardiac fibrosis were increased in the heart of hypertension-resistant (HR), hypertension-prone (HP), and hypertension (HTN) rats on HSD by Masson's staining. B, The mRNA levels of collagen I, alpha-smooth muscle actin (α-SMA) and transforming growth factor-beta (TGF-β) were increased in the heart of HR, HP and HTN rats on HSD. C, The protein levels of collagen I, α-SMA and TGF-β were increased in the heart of HR, HP and HTN rats on

HSD. The results are expressed as mean ± standard error of the mean (SEM); n=8 in each group. *p<0.05, **p<0.01, ***p<0.001, and ****p<0.0001.

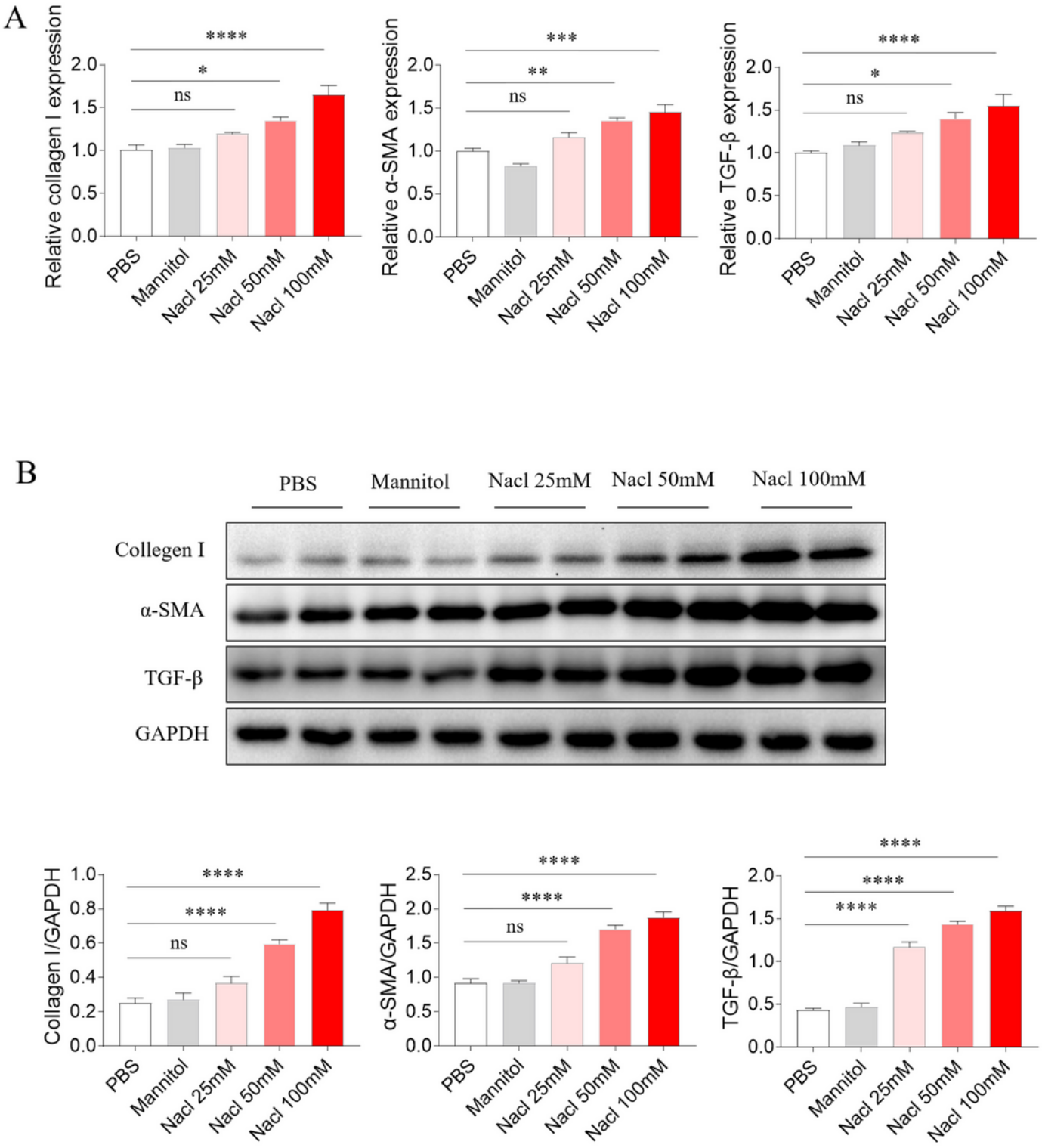

Figure 2

Effects of sodium chloride (NaCl) on the fibrosis of neonatal rat cardiac fibroblasts (NRCFs). A, Middle (50 mM) and high (100 mM) doses of NaCl increased the mRNA levels of collagen I, alpha-smooth muscle actin (α-SMA) and transforming growth factor-beta (TGF-β) in NRCFs. B, Middle (50 mM) and

high (100 mM) doses of NaCl increased the protein levels of collagen I, α-SMA and TGF-β in NRCFs. The results are expressed as mean ± standard error of the mean (SEM); n=6 in each group. *p<0.05, **p<0.01, ***p<0.001, and ****p<0.0001.

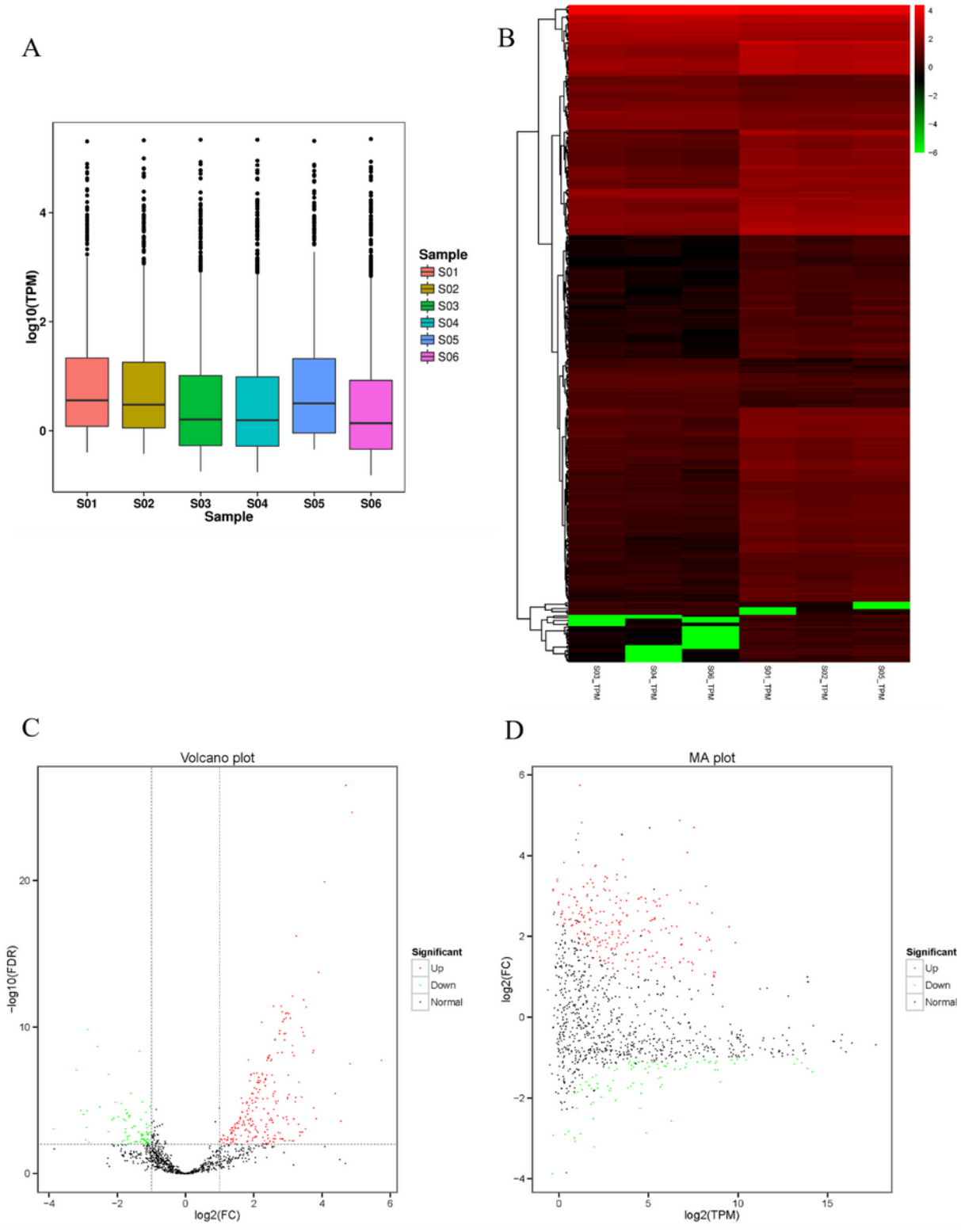

Figure 3

The differentially expressed microRNAs (miRs) between NaCl and control groups determined by small RNA sequencing. A, The box-plot of the samples. The horizontal axis represents different samples, and

the vertical axis represents the logarithm of Transcripts Per Million (TPM). B, The heat map of differentially expressed miRs among samples (|FC|>=2, FDR (False Discovery Rate) <0.01); the horizontal axis represents different samples, and the vertical axis represents miRs. In the figure, red indicates a positive correlation, and green indicates a negative correlation. The deeper color indicates a greater correlation. C, The volcano plot of differentially expressed miRs among samples (|FC|>=2, FDR<0.01). Each point represents a miR. The horizontal axis represents the logarithm of the differential expression multiple of a miRNA between two samples, and the horizontal axis represents the negative logarithm of FDR. D, The M-versus-A (MA) plot of differentially expressed miRs among samples. The red dots represent up-regulated miRs, the green dots represent down-regulated miRs, and the black dots represent non-differentially expressed miRs.

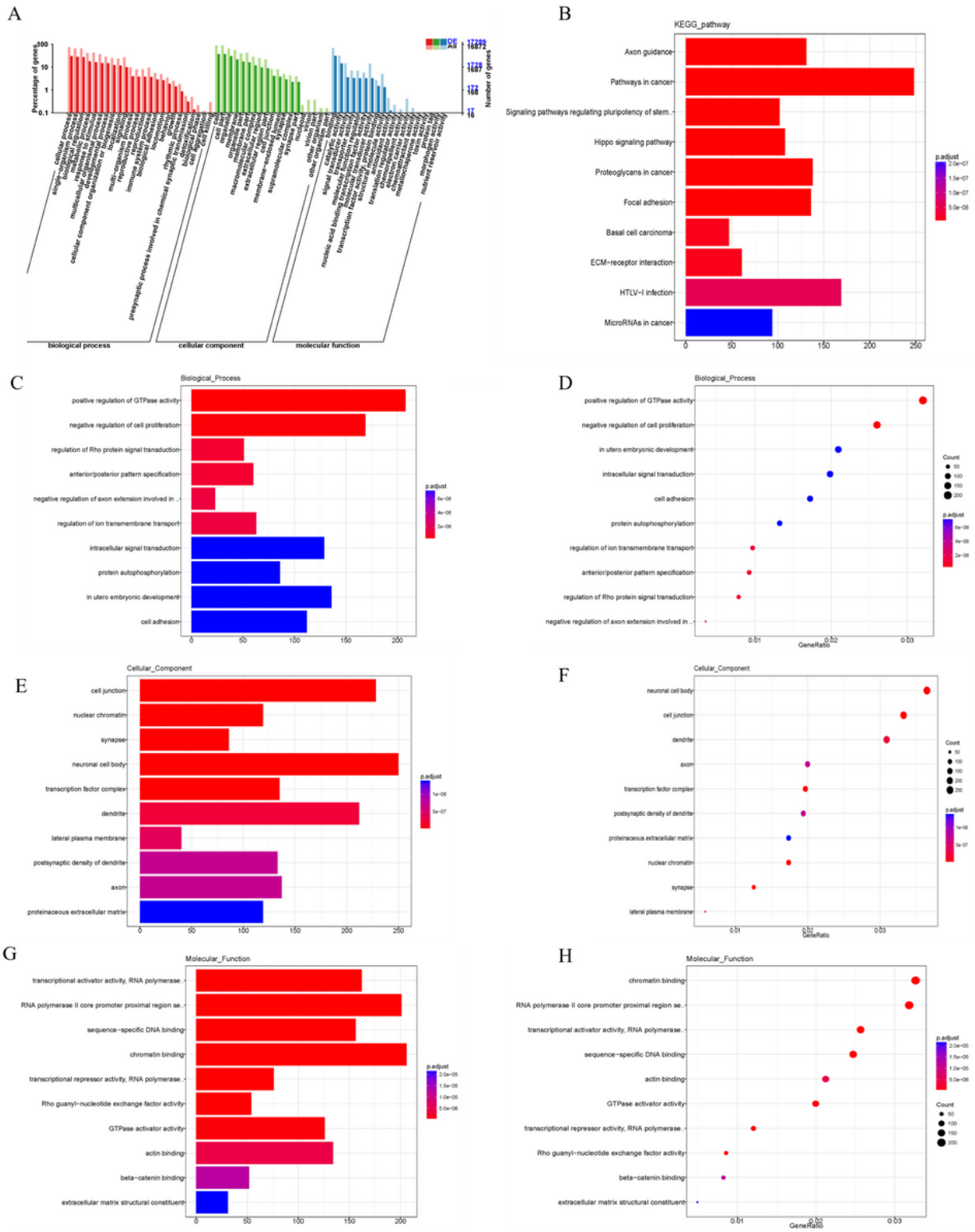

Figure 4

Functional analysis of target genes of differentially expressed microRNAs (miRs). A, The correlation GO analysis. B, The top 10 enriched terms of KEGG pathway. C and D, The enriched barplot (C) and dotplot (D) of top 10 enriched terms of biological process. E and F, The enriched barplot (E) and dotplot (F) of top 10 enriched terms of molecular function. G and H, The enriched barplot (G) and dotplot (H) of top 10 enriched terms of cellular component. The size of the dot represents the number of target genes of the

differentially expressed miR. The bigger size indicates more genes. The color of the dot represents the corrected P-value of the hypergeometric test; the darker color means a smaller P-value.

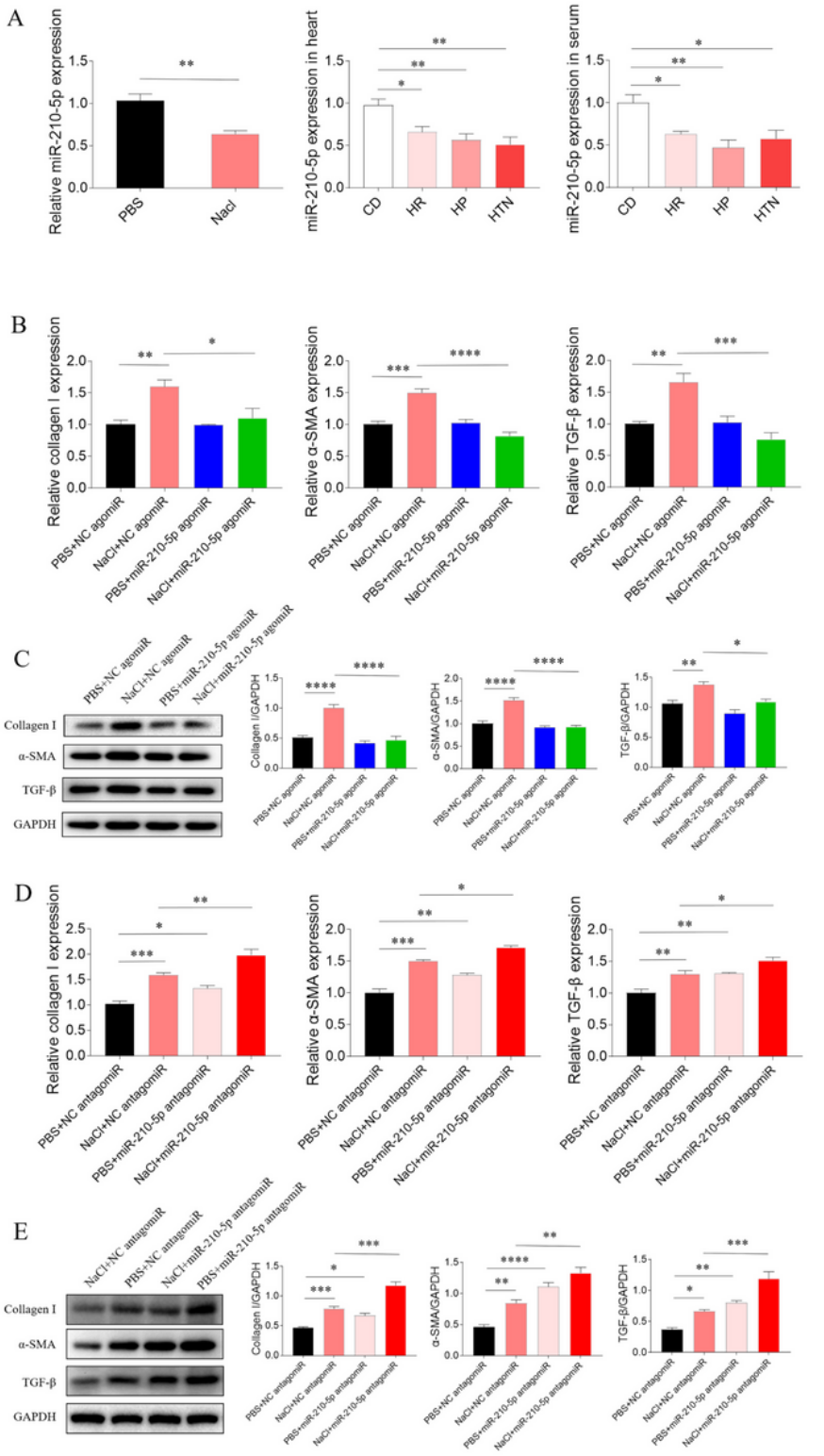

Figure 5

Effects of microRNA (miR)-210-5p on the neonatal rat cardiac fibroblasts (NRCFs) fibrosis induced by NaCl. A, The expression levels of miR-210-5p were reduced in NaCl-treated NRCFs, and in the heart and serum of hypertension-resistant (HR), hypertension-prone (HP) and hypertension (HTN) rats fed with high

salt diet (HSD). B, Treatment with miR-210-5p agomiR inhibited the increases of mRNA levels of collagen I, alpha-smooth muscle actin (α-SMA) and transforming growth factor-beta (TGF-β) induced by NaCl in NRCFs. C, Treatment with miR-210-5p agomiR inhibited the increases of protein levels of collagen I, α-SMA and TGF-β induced by NaCl in NRCFs. D, Treatment with miR-210-5p antagomiR further enhanced the increases of mRNA levels of collagen I, α-SMA and TGF-β induced by NaCl in NRCFs. E, Treatment with miR-210-5p antagomiR further enhanced the increases of protein levels of collagen I, α-SMA and TGF-β induced by NaCl in NRCFs. The results are expressed as mean ± standard error of the mean (SEM); n=6 in each group. *p<0.05, **p<0.01, ***p<0.001, and ****p<0.0001.

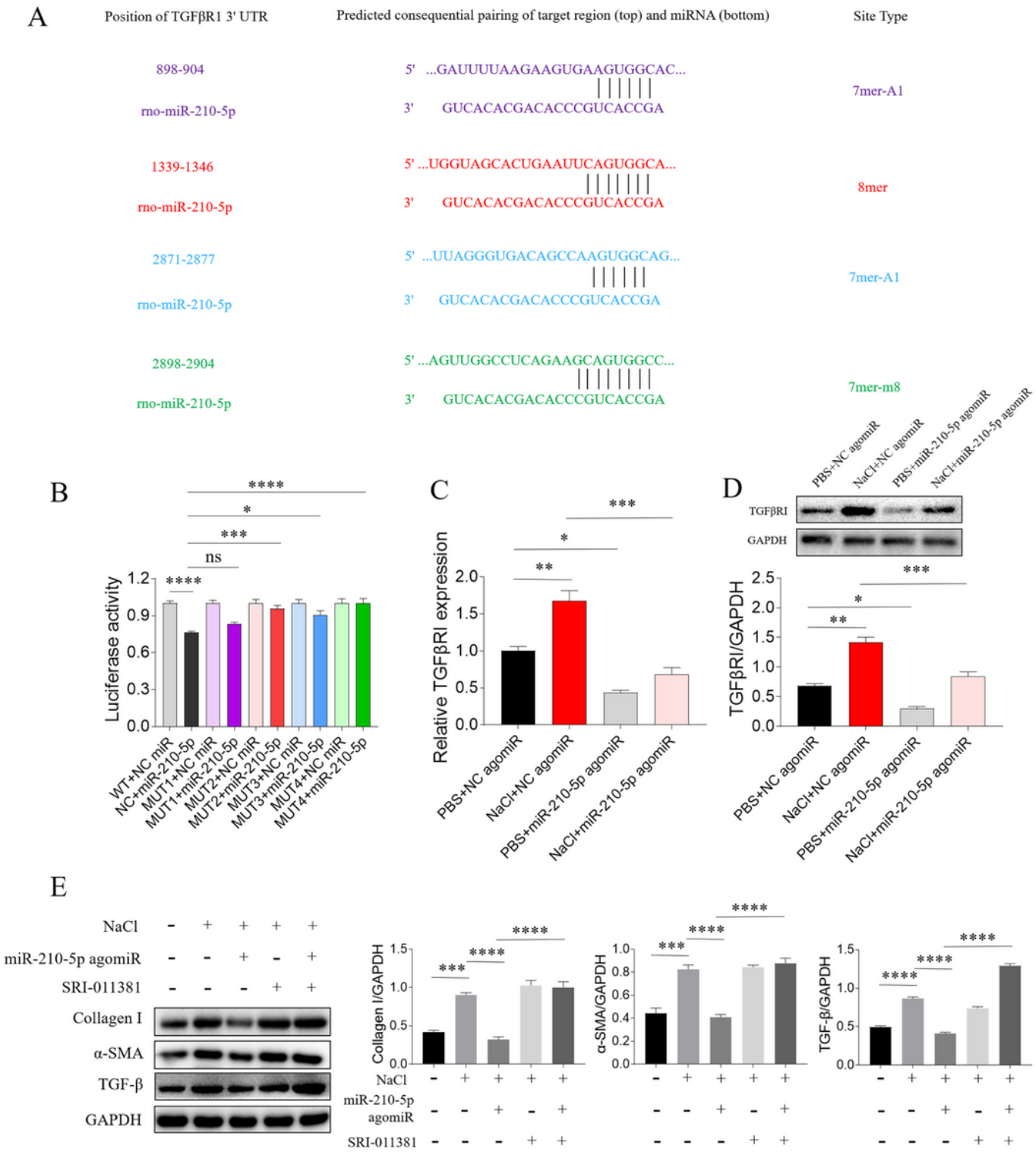

Figure 6

The target of microRNA (miR)-210-5p. A, The four predicted binding sites of miR-210-5p in the 3' UTR region with transforming growth factor beta1 receptor (TGFβ1R). B, MiR-210-5p decreased the luciferase activities of the vector with wild type TGFβ1R 3'UTR, and this decrease was attenuated by TGFβ1R MUT2 (1339-1346, 19.52%), TGFβ1R MUT3 (2871-2877, 14.41%) and TGFβ1R MUT4 (2898-2904, 23.73%). C, TGFβ1R mRNA level was increased in NaCl-treated NRCFs, and this increase was inhibited by miR-210-5p

agomiR. D, TGFβ1R protein level was increased in NaCl-treated NRCFs, and this increase was inhibited by miR-210-5p agomiR. E, SRI-011381, an activator of TGF-β signaling pathway, reversed the attenuating effects of miR-210-5p on the increases of collagen I, α-SMA and TGF-β induced by NaCl in NRCFs. The results are expressed as mean ± standard error of the mean (SEM); n=6 in each group. *p<0.05, **p<0.01, ***p<0.001, and ****p<0.0001.

Supplementary Files

This is a list of supplementary files associated with this preprint. Click to download.

- FigureS3.png
- FigureS2.png
- FigureS1.png
- TableS1.doc
- TableS2.doc